The EMBO Journal Vol.18 No.8 pp.2184–2195, 1999

The disappearance of cyclin B at the end of mitosis is regulated spatially in *Drosophila* cells

Jun-yong Huang and Jordan W.Raff[1]

Wellcome/CRC Institute and Department of Genetics, University of Cambridge, Tennis Court Road, Cambridge CB2 1QR, UK

[1]Corresponding author
e-mail: j.raff@welc.cam.ac.uk

We have followed the behaviour of a cyclin B–green fluorescent protein (GFP) fusion protein in living *Drosophila* embryos in order to study how the localization and destruction of cyclin B is regulated in space and time. We show that the fusion protein accumulates at centrosomes in interphase, in the nucleus in prophase, on the mitotic spindle in prometaphase and on the microtubules that overlap in the middle of the spindle in metaphase. In cellularized embryos, toward the end of metaphase, the spindle-associated cyclin B–GFP disappears from the spindle in a wave that starts at the spindle poles and spreads to the spindle equator; when the cyclin B–GFP on the spindle is almost undetectable, the chromosomes enter anaphase, and any remaining cytoplasmic cyclin B–GFP then disappears over the next few minutes. The endogenous cyclin B protein appears to behave in a similar manner. These findings suggest that the inactivation of cyclin B is regulated spatially in *Drosophila* cells. We show that the anaphase-promoting complex/cyclosome (APC/C) specifically interacts with microtubules in embryo extracts, but it is not confined to the spindle in mitosis, suggesting that the spatially regulated disappearance of cyclin B may reflect the spatially regulated activation of the APC/C.

Keywords: anaphase-promoting complex/cyclin B/*Drosophila*/mitotic spindle/protein degradation

Introduction

The sequential activation and inactivation of cyclin-dependent protein kinases (cdks) ensures the proper timing and order of cell cycle events. The complex of cdk1 (cdc2) and cyclin B is the main regulator of the entry into mitosis, and multiple factors control its activity (Harper and Elledge, 1996; King *et al*., 1996; Lew and Kornbluth, 1996). The destruction of cyclin B via the polyubiquitination pathway (Glotzer *et al*., 1991), however, normally is required for the inactivation of the complex and the exit from mitosis (Murray, 1995). This destruction is initiated by the anaphase-promoting complex, or cyclosome (APC/C), which ubiquitinates cyclin B at the metaphase–anaphase transition (Hershko *et al*., 1994; Irniger *et al*., 1995; King *et al*., 1995). The APC/C also ubiquitinates several other proteins during mitosis (CohenFix *et al*., 1996; Funabiki *et al*., 1996; Juang *et al*., 1997; Michaelis *et al*., 1997; Charles *et al*., 1998; Shirayama *et al*., 1998). By targeting specific proteins for destruction at specific times during mitosis, the APC/C plays a crucial role in orchestrating the late events of mitosis (reviewed in Townsley and Ruderman, 1998).

Although the destruction of cyclin B clearly is regulated temporally, it is not known whether it is also regulated spatially in dividing cells. Recent studies on cells arrested in mitosis by the spindle assembly checkpoint, however, suggest that at least some aspects of the exit from mitosis can be regulated spatially in cells. This checkpoint monitors the fidelity of the spindle and arrests the cell cycle prior to the destruction of cyclin B if the spindle is not assembled correctly (reviewed in Wells, 1996). In fused tissue culture cells containing two spindles, the activation of the checkpoint in one spindle (by the presence of an unattached kinetochore) arrests that spindle in metaphase, but does not block the other spindle from exiting mitosis and entering anaphase with normal timing (Rieder *et al*., 1997). This finding suggests that the exit from mitosis can be controlled locally.

Previous studies on the early *Drosophila* embryo suggested that cyclin B degradation might be regulated spatially in cells. After fertilization, these embryos undergo a series of 13 rapid nuclear divisions in a common cytoplasm. Although the destruction of cyclin B is required for the exit from mitosis in these embryos (Su *et al*., 1998), biochemical studies have shown that cyclin B is only partially degraded at the end of each round of mitosis during these syncytial cycles, and it has been suggested that the degradation might be restricted spatially to the areas around the chromosomes or spindles (Edgar *et al*., 1994). In support of this suggestion, fractions of cyclin B and cdk1 are associated with centrosomes, spindles and chromatin during mitosis in several systems (Riabowol *et al*., 1989; Alfa *et al*., 1990; Pines and Hunter, 1991; Debec and Montmory, 1992; Maldonado-Codina and Glover, 1992), and fractions of the APC/C are associated with centrosomes, spindles and centromeres in mammalian cells (Tugendreich *et al*., 1995; Jorgensen *et al*., 1998).

It is not clear, however, how cyclin B is only partially degraded in syncytial *Drosophila* embryos. While immunofluorescent studies on fixed cellularized embryos showed that cyclin B is degraded completely at the end of mitosis in the cells of these embryos (Lehner and O'Farrell, 1990; Whitfield *et al*., 1990), similar studies on syncytial embryos failed to detect a clear-cut destruction of cyclin B at the end of mitosis (Maldonado-Codina and Glover, 1992). As these authors noted, however, the distribution of cyclin B in syncytial embryos is dependent crucially on fixation conditions, suggesting that the distribution of cyclin B in the fixed syncytial embryos may not reflect accurately the distribution of the protein in living embryos.

To circumvent the potential problems associated with fixation, we have expressed a cyclin B–green fluorescent protein (GFP) fusion protein in *Drosophila* embryos, allowing us, for the first time, to follow the distribution and destruction of cyclin B throughout the cell cycle in a living system. We show that the distribution of cyclin B–GFP is highly dynamic, and its disappearance at the end of mitosis is regulated both temporally and spatially. The spatial regulation probably explains the previous biochemical findings that cyclin B is only partially destroyed in syncytial embryos. These results may have important implications for how the exit from mitosis is controlled.

Results

Cyclin B–GFP is degraded with normal kinetics in early Drosophila embryos

To visualize the distribution and destruction of cyclin B directly during the cell cycle, we expressed a cyclin B–GFP fusion protein in *Drosophila* embryos using the polyubiquitin promoter, which is expressed at high levels at all stages of fly development (Lee *et al*., 1988). Flies transformed with this construct appeared to be healthy and, in 2- to 4-h-old embryos that carried four copies of the cyclin B–GFP transgene, the fusion protein was expressed at about half the level of the endogenous cyclin B protein (Figure 1A).

To test whether the cyclin B–GFP protein was destroyed at the end of mitosis, we fixed cyclin B–GFP-expressing embryos with methanol and determined their cell cycle stage by staining their DNA. Twenty embryos at various stages of nuclear cycle 10–11 were pooled and boiled in sample buffer, and the behaviour of cyclin B and cyclin B–GFP was analysed by Western blotting (Figure 1B). Quantitation of these blots showed that both proteins accumulated to the same extent between interphase and early metaphase, and were partially degraded to the same extent as embryos exited mitosis.

The distribution and destruction of cyclin B–GFP during the cell cycle in living cellularized embryos

We followed the distribution and disappearance of the cyclin B–GFP fusion protein in living cellularized embryos, where cell division occurs in a well-defined pattern of mitotic domains (Foe, 1989). Figure 2A shows a low magnification view of the dorsal side of an embryo, where cells in the first mitotic domains were about to enter mitosis (arrows at 0.0 min); by 6.40 min, most of the cells in these domains had exited mitosis, and the fluorescent signal had disappeared. As the endogenous cyclin B protein previously has been shown to disappear from these cells at about the metaphase–anaphase transition (Lehner and O'Farrell, 1990; Whitfield *et al*., 1990), it seems likely that this loss of fluorescence reflects the degradation of the cyclin B–GFP.

Figure 2B shows a higher magnification view of a small group of cells at different stages of the cell cycle and follows one cell (marked with an arrow) through mitosis. At 0.0 min, the cells in the bottom left of the panel were in interphase of cycle 14 (i), and the cyclin B–GFP was located mainly in the cytoplasm, with small amounts at the centrosomes. The cells at the top and right of the

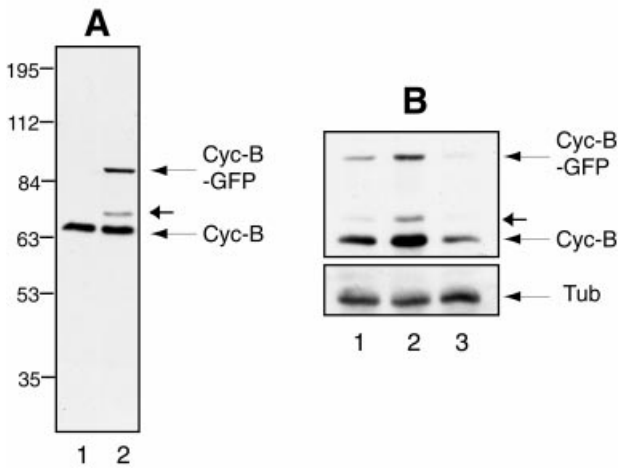

Fig. 1. (**A**) Western blot of embryo extracts probed with affinity-purified anti-cyclin B antibodies. In 2- to 4-h-old wild-type embryos (lane 1), the antibodies recognize a single major band of ~65 kDa. In 2- to 4-h-old transgenic embryos expressing four copies of the cyclin B–GFP transgene (lane 2), an extra band of ~90 kDa is detected, which was also detected with anti-GFP antibodies (not shown). A smaller protein that is presumably a breakdown product of cyclin B–GFP is also present in this lane (small arrow); this protein was not detected by two different anti-GFP monoclonal antibodies (not shown) and it was degraded at the end of mitosis (see below), suggesting that it contains a destruction box, but is missing some GFP sequences. Thus, we do not think it interferes with the interpretation of our results. (**B**) Western blot of nuclear cycle 10 embryos at different stages of the cell cycle probed with anti-cyclin B antibodies. Lane 1, embryos in early interphase; lane 2, embryos in prometaphase/early metaphase; lane 3, embryos in anaphase/telophase. Quantitation of this blot shows that cyclin B, cyclin B–GFP and the cyclin B–GFP breakdown product (small arrow) all accumulate to the same extent from interphase to metaphase, and are all partially degraded to the same extent as embryos exit mitosis. This blot was probed with an anti-α-tubulin antibody as a loading control.

panel were in different stages of mitosis (m). The two cells marked with an asterisk were in late mitosis, and cyclin B–GFP fluorescence was hardly detectable. The cell marked with an arrow was just about to enter mitosis, and we describe the subsequent behaviour of this cell.

At time 0.0, just prior to the entry into mitosis, the level of cyclin B–GFP at the centrosomes of this cell had increased (compare this arrowed cell with other cells in interphase in Figure 2B, 0.0). A significant fraction of the cytoplasmic cyclin B–GFP then rapidly accumulated in the nucleus (Figure 2B, 0.42), the nuclear envelope broke down and the majority of the nuclear fusion protein appeared to relocate to the forming mitotic spindle (Figure 2B, 1.45). In metaphase, the protein at each centrosome became focused in a small dot, and the spindle-associated protein accumulated at the ends of the interpolar microtubules that overlapped in the middle region of the spindle (Figure 2B, 2.13; the co-localization with this subset of microtubules is seen more easily in fixed embryos; see Figures 4A and 6C, D). This pattern persisted throughout metaphase, which was of variable length. Just prior to the initiation of anaphase, the cyclin B–GFP on the mitotic spindle disappeared over a period of ~1–2 min (Figure 2B, 3.09–4.12). In time-lapse movies, the disappearance of the fusion protein appeared to start in the region of the spindle poles and then spread rapidly toward the spindle equator. This is hard to illustrate in still images (see also Figure 4B, arrowed spindle;

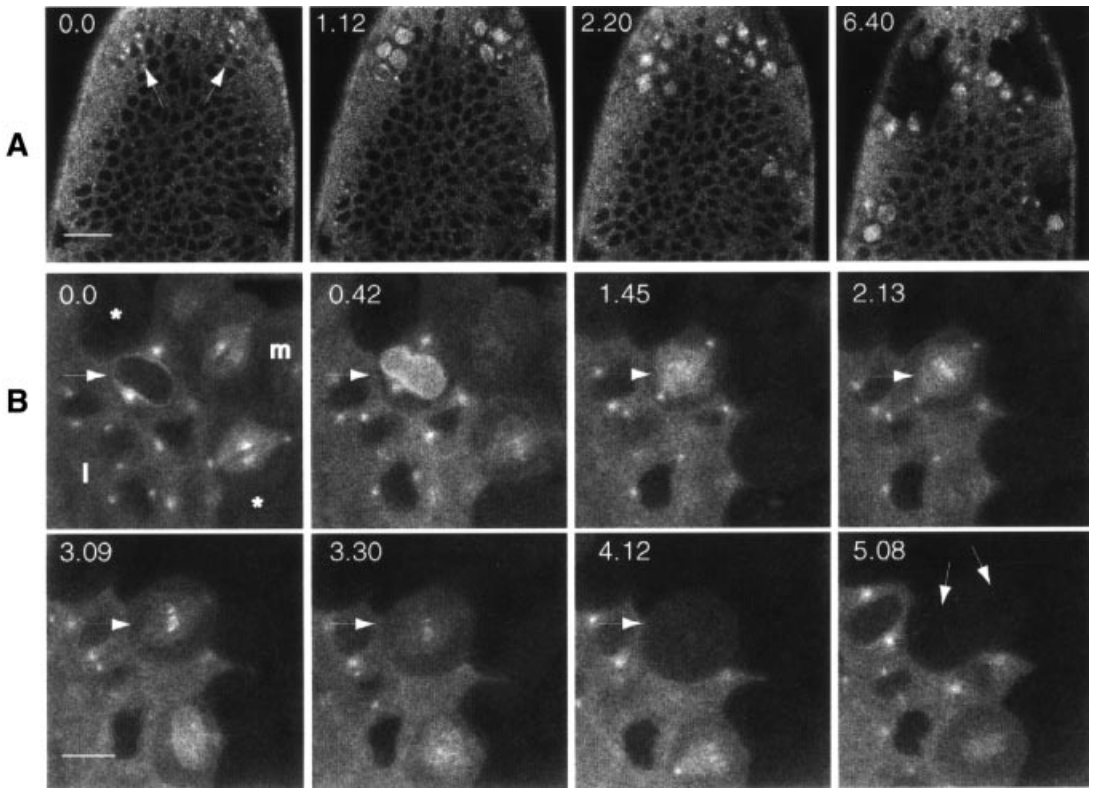

Fig. 2. Confocal fluorescence micrograph showing the distribution of cyclin B–GFP in living cellularized embryos. The time in minutes is shown in the upper left hand corner of each panel. (**A**) Low magnification views of the dorsal side of an embryo, where cells in the first mitotic domains are about to enter mitosis (arrows 0.0 min). At 6.40 min, most of the cells in these domains have exited mitosis and have destroyed their cyclin B–GFP. Scale bar = 30 μm. (**B**) High magnification view of a group of cells. At 0.0 min, different cells are at different stages of the cell cycle. The arrowed cell at 0.0 min is about to enter mitosis; the distribution of cyclin B–GFP in this cell is described in the text. Scale bar = 5 μm.

movies of this process can be downloaded from http://www.welc.cam.ac.uk/~rafflab/Movies/).

At about the time the cyclin B–GFP on the spindle disappeared, the cells entered anaphase (the separating chromosomes could be seen as two darker areas in the cell, arrowed at time 5.08), and any fluorescence that remained in the cytoplasm then disappeared over the next few minutes. As the cells initiated cytokinesis (Figure 2B, 5.08), the level of fluorescence in the cytoplasm still had not dropped to its lowest level (compare the level of cytoplasmic fluorescence in the marked cell with that of the cells that were completing mitosis at time 0.0, top and right of panel).

To test whether the disappearance of the cyclin B–GFP from the spindle was due to the degradation or the redistribution of the protein, we quantified the fluorescence in the various regions of the cell (Figure 3). As the cell prepared to enter mitosis, ~30% of the fluorescence disappeared from the cytoplasm and appeared to accumulate in the nucleus. As the nuclear envelope broke down, however, there was no increase in the level of fluorescence in the cytoplasm, and the bulk of the nuclear fluorescence appeared to relocate to the forming mitotic spindle. The level of fluorescence in the cytoplasm remained relatively constant even as the fluorescence disappeared from the spindle, and it reproducibly started to fall even before all of the signal from the spindle was gone. This suggested that some cyclin B–GFP was being degraded in the cell at the same time as the protein was disappearing from the spindle. Qualitatively similar results were obtained in two other cells that were quantified in this way (not shown).

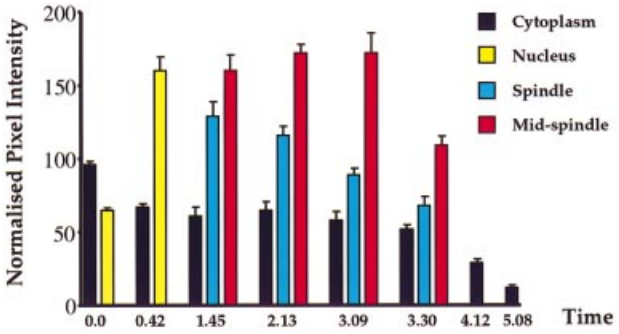

Fig. 3. Quantitation of cyclin B–GFP fluorescence at various locations in the cell. The time on the *x*-axis is in minutes and correlates with the times shown in Figure 2B. The *y*-axis represents a normalized mean pixel intensity (see Materials and methods). Error bars represent the standard deviation.

The distribution and destruction of the endogenous cyclin B protein in cellularized embryos

This behaviour of cyclin B–GFP in living embryos is very different from that reported for cyclin B in formaldehyde-fixed embryos, where cyclin B is largely distributed in the cytoplasm, and abruptly disappears at about the time of the metaphase–anaphase transition (Lehner and O'Farrell, 1990; Whitfield *et al*., 1990). To test whether the behaviour of cyclin B–GFP accurately reflected the behaviour of the endogenous cyclin B, we raised and affinity-purified antibodies against *Drosophila* cyclin B. These purified antibodies recognized a single major band on Western

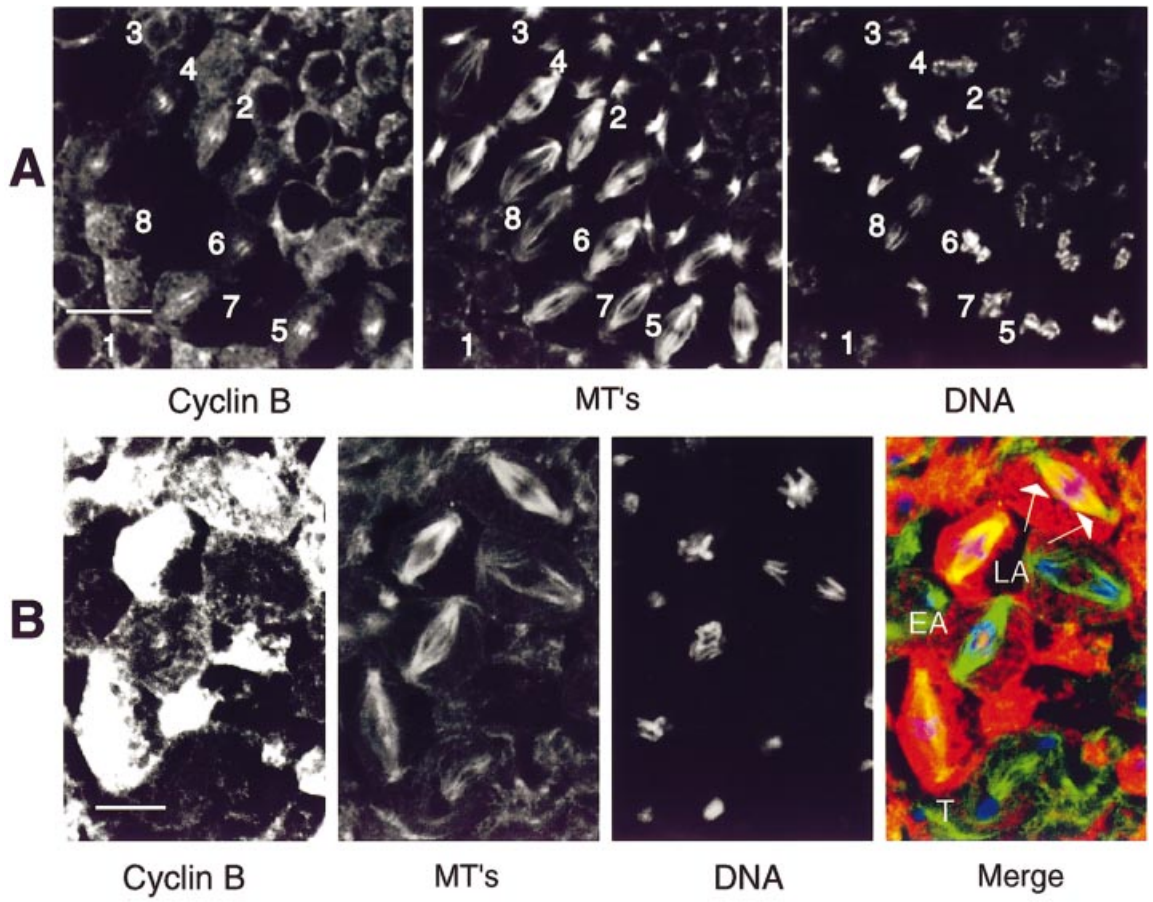

Fig. 4. The distribution of endogenous cyclin B protein in methanol-fixed embryos. (**A**) A mitotic domain in a cellularized embryo. Cyclin B is stained in the left panel, microtubules in the middle panel and DNA in the right panel. Cells at different stages of the cell cycle are marked with numbers that refer to the cell directly to the right of the number (see text for details). (**B**) A mitotic domain in a cellularized embryo where the gain of the cyclin B channel has been increased to allow the behaviour of the cyclin B in the cytoplasm to be followed more easily. Letters refer to the cell on their right in the merged image: EA = early anaphase; LA = late anaphase; T = telophase. In the merged image, cyclin B is red, microtubules are green and DNA is blue. Arrows show the cyclin B starting to disappear from the spindle poles in a cell in metaphase. Scale bar (A) = 10 μm, (B) = 5 μm.

blots of whole embryo extracts (Figure 1), which ran at the expected size of cyclin B (Lehner and O'Farrell, 1990; Whitfield *et al*., 1990).

In formaldehyde-fixed cellularized embryos, these antibodies revealed a similar distribution of cyclin B to that reported previously (not shown). In methanol-fixed cellularized embryos, however, these antibodies had a very similar distribution pattern to that observed with cyclin B–GFP in living embryos (Figure 4A). In interphase, the cyclin B was predominantly cytoplasmic (Figure 4A, cell #1), with a small amount concentrated at centrosomes (not shown). In early prophase, cyclin B accumulated at the centrosomes (cell #2) and prior to nuclear envelope breakdown it moved into the nucleus (cells #3 and #4). At metaphase, it became concentrated on the plus ends of the interpolar microtubules that overlapped in the middle of the spindle (cell #5). In late metaphase, the protein on the spindle started to disappear from the spindle poles (cell #6), and by early anaphase it was almost completely gone from the spindle (cell #7). In mid-anaphase, virtually no cyclin B was detectable in the cell (cell #8). The amount of cyclin B detectable in the cytoplasm during mitosis was often difficult to judge in fixed embryos, as methanol fixation caused the cells to shrink slightly and lose their normal shape, creating gaps in the cell layer. Thus it was difficult to tell whether any of the endogenous cyclin B protein remained in the cytoplasm and was only destroyed during the latter stages of mitosis (as seen with cyclin B–GFP in living embryos). If we increased the sensitivity of detection, however, cyclin B was detectable reproducibly in the cytoplasm of methanol-fixed cells during mitosis, and it gradually disappeared from the cells as they progressed through late mitosis [compare the cytoplasmic staining in the cells in early anaphase (EA), late anaphase (LA) and telophase (T) in Figure 4B].

Thus, the behaviour of endogenous cyclin B (visualized in methanol-fixed cells) and cyclin B–GFP (visualized in living cells) was very similar. The only significant difference was that the accumulation of cyclin B in the nucleus prior to nuclear envelope breakdown (NEB) and on the centrosomes during mitosis was less pronounced in methanol-fixed embryos. To address why the distribution of cyclin B–GFP in living embryos is slightly different from the distribution of the endogenous cyclin B in methanol-fixed embryos, and is very different from the distribution of the endogenous cyclin B in formaldehyde-fixed embryos, we fixed cyclin B–GFP-expressing embryos with either formaldehyde or methanol. We then stained them with anti-cyclin B antibodies to see if fixation had effected the distribution of the cyclin B–GFP protein.

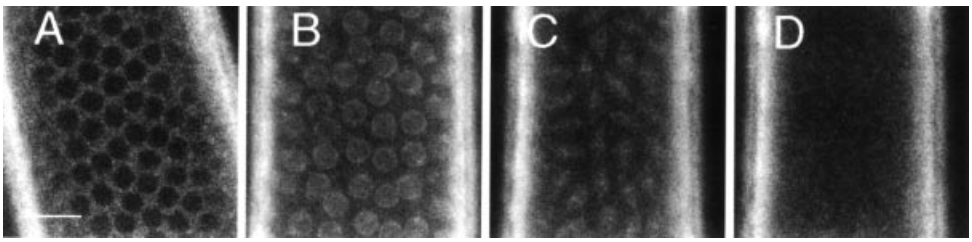

Fig. 5. The localization of cyclin B–GFP in living syncytial embryos. (**A**) An embryo in interphase. Cyclin B–GFP is predominantly cytoplasmic but is also present in the centrosomes (which are only partly visible in this plane of focus). (B–D) A single embryo followed through mitosis. In prometaphase (**B**), the cyclin B–GFP is largely in the nucleus; it is also present in centrosomes which are only partly visible in this plane of focus. In metaphase (**C**), the protein is concentrated in the middle of the spindle, on centrosomes, and it is also present on the rest of the spindle. This pattern persisted for ~40 s before the fluorescence on the spindles rapidly disappeared (**D**), presumably because the embryo exited mitosis. Scale bar = 30 μm.

The distribution of the cyclin B and cyclin B–GFP in these fixed embryos was indistinguishable from the distribution of cyclin B in similarly fixed wild-type embryos (not shown), suggesting that the cyclin B–GFP protein is redistributed subtly upon methanol fixation, and is redistributed drastically upon formaldehyde fixation. We have also performed these experiments with several commercially available anti-GFP antibodies, but none of these detected GFP very well in methanol-fixed embryos (not shown).

Cyclin B–GFP in syncytial embryos

To determine why previous biochemical studies had found that cyclin B is only partially degraded at the end of mitosis in syncytial embryos (Edgar *et al*., 1994), we tried to study the distribution and degradation of cyclin B–GFP in these embryos. We found, however, that it was impossible to get high resolution images of cyclin B–GFP in these embryos as the fluorescent signal was too low, even when we produced embryos that expressed cyclin B–GFP from the maternal 67C α-tubulin promoter, which is expressed at very high levels during oogenesis (Micklem *et al*., 1997).

Although the fluorescent signal was low, the distribution of cyclin B–GFP in syncytial embryos appeared to be similar to that seen in cellularized embryos, and the spindle-associated fraction of the protein clearly disappeared toward the end of metaphase (Figure 5). Because the low signal made it hard to follow accurately the disappearance of the cyclin B–GFP at the end of mitosis, we followed the behaviour of endogenous cyclin B in immunostained methanol-fixed syncytial embryos (Figure 6). Previous studies on formaldehyde-fixed syncytial embryos failed to find a clear-cut disappearance of cyclin B (Maldonado-Codina and Glover, 1992). We found, however, that in methanol-fixed syncytial embryos, the behaviour of endogenous cyclin B was very similar to that seen with cyclin B–GFP in living cellularized embryos, and the spindle-associated fraction of the cyclin B started to disappear from the spindle poles in late metaphase (compare Figure 6C with D), and was essentially absent from the spindles by anaphase (Figure 6E). In contrast to the situation in fixed cellularized embryos (Figure 4), the majority of cyclin B staining in the cytoplasm of syncytial embryos did not disappear during mitosis (compare Figure 6C with E), and the cytoplasmic staining remained essentially constant as the embryos progressed through telophase and into the next interphase (not shown). Thus, only the cyclin B in the vicinity of the spindle disappears at the end of mitosis in syncytial embryos.

The Drosophila APC/C associates with microtubules in embryo extracts, but is present at multiple locations within the embryo

It has been reported previously that the APC/C is concentrated on centrosomes and spindles in mammalian cells (Tugendreich *et al*., 1995). If this were also the case in *Drosophila* embryos, it might explain how the disappearance of cyclin B is initiated on the spindles in these embryos. To study the distribution of the APC/C in *Drosophila* embryos, we cloned a cDNA that encodes the *Drosophila* homologue of the APC/C component cdc16 (Dmcdc16). We then raised and affinity-purified antibodies against the Dmcdc16 protein, as well as against the previously described *Drosophila* homologue of the APC/C component cdc27 (Dmcdc27; S.Tugendreich and P.Hieter, personal communication).

We raised and purified antibodies against two regions of the Dmcdc27 protein, and a single region of the Dmcdc16 protein. In Western blots of embryo extracts, both of the antibodies raised against the Dmcdc27 protein recognized a prominent band of ~100 kDa, which is close to the predicted size (102 kDa) of the Dmcdc27 protein, as well as a number of other bands (Figure 7A). Only the 100 kDa protein was co-precipitated with the anti-Dmcdc16 antibodies (Figure 7B). The anti-Dmcdc16 antibodies recognized a prominent band of ~80 kDa, which is close to the predicted size (82 kDa) of the Dmcdc16 protein, as well as a band of ~58 kDa (Figure 7A). Only the ~80 kDa protein was co-precipitated with anti-Dmcdc27 antibodies (Figure 7B). In sucrose gradient sedimentation experiments, fractions of the Dmcdc16 and Dmcdc27 proteins appeared to co-migrate as a large complex (>19S), although a large fraction of the Dmcdc16 protein behaved as a much smaller protein (Figure 7C); a similar result has been reported previously for the cdc16 homologue *cut9* in *Schizosaccharomyces pombe* (Yamada *et al*., 1997). These results suggest that Dmcdc16 and Dmcdc27 are both components of the same higher molecular weight complex, presumably the *Drosophila* APC/C.

We tested whether these proteins interacted biochemically with microtubules by performing microtubule spin-down experiments with early embryo extracts. We found that the majority of the Dmcdc27, and a substantial fraction of Dmcdc16, interacted with microtubules

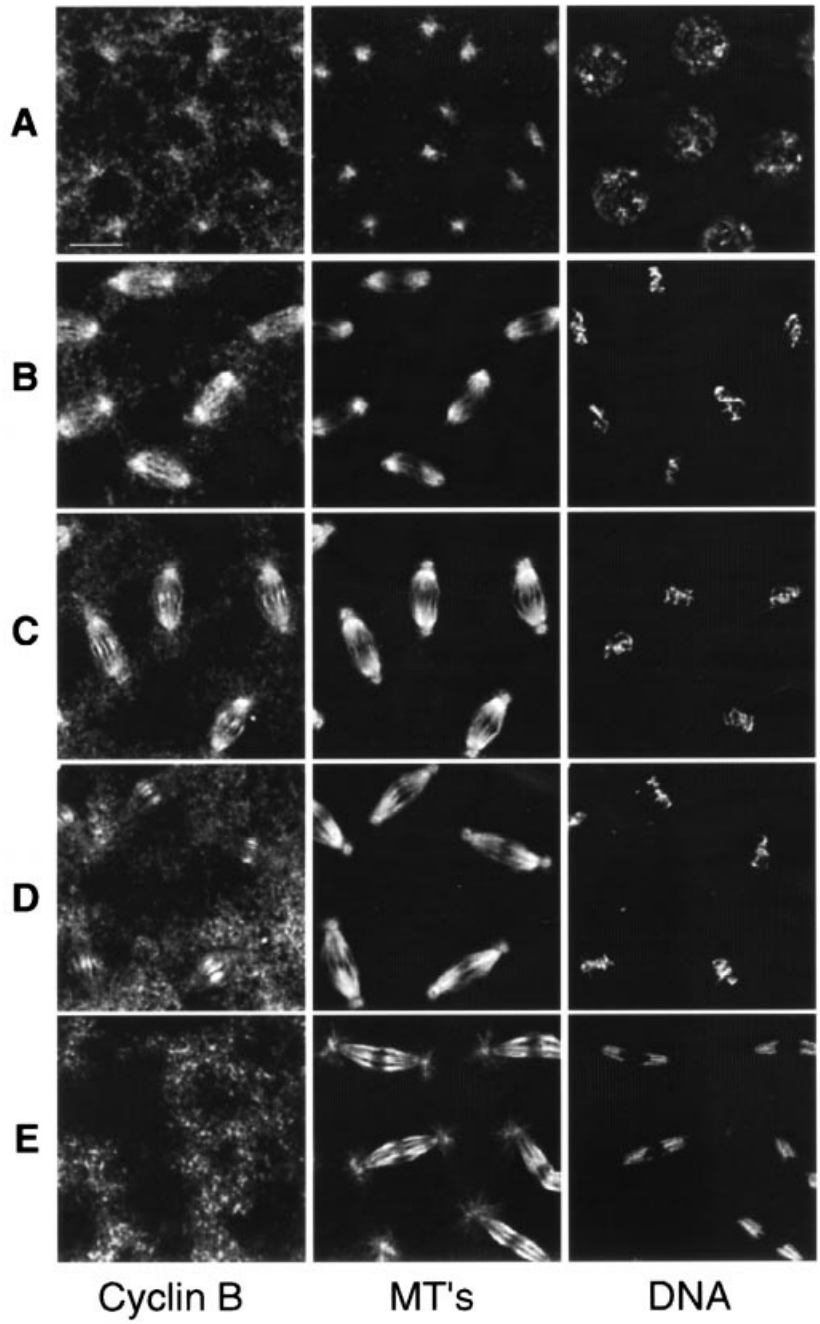

Fig. 6. The distribution of endogenous cyclin B in methanol-fixed syncytial embryos. Left hand panels, cyclin B; middle panels, microtubules; right hand panels, DNA. (**A**) Interphase; (**B**) early metaphase; (**C**) metaphase; (**D**) late metaphase; (**E**) anaphase. Cyclin B initially is concentrated at the poles of the forming spindle (B) and then becomes concentrated on the microtubules that overlap in the middle of the spindle, although it is still present at the poles (C). The spindle-associated cyclin B starts to disappear from the spindle poles in late metaphase (D). The disappearance spreads to the rest of the spindle so that by anaphase (E), almost no cyclin B is present in the spindle. Cytoplasmic cyclin B, in contrast, remains essentially constant throughout the cell cycle. Scale bar = 10 μm.

(Figure 7D). The majority of cyclin B also interacted with microtubules in this type of experiment. The interaction of these proteins with microtubules appeared to be specific, as none of them associated with actin filaments polymerized in similar extracts (Figure 7D).

When we used the anti-Dmcdc16 and anti-Dmcdc27 antibodies to stain syncytial *Drosophila* embryos, however, they only weakly labelled centrosomes and microtubules in methanol-fixed embryos (Figure 8). A weak punctate staining was also visible in the chromosomal regions during mitosis, but the bulk of the Dmcdc16 and Dmcdc27 appeared to be distributed in a punctate fashion throughout the cytoplasm at all stages of the cell cycle. Thus, the APC/C appears to be located at multiple sites within the embryo.

Discussion

We have used a cyclin B–GFP fusion protein to follow the distribution and destruction of cyclin B through the entire cell cycle in living *Drosophila* embryos. We find that the distribution of cyclin B–GFP is highly dynamic,

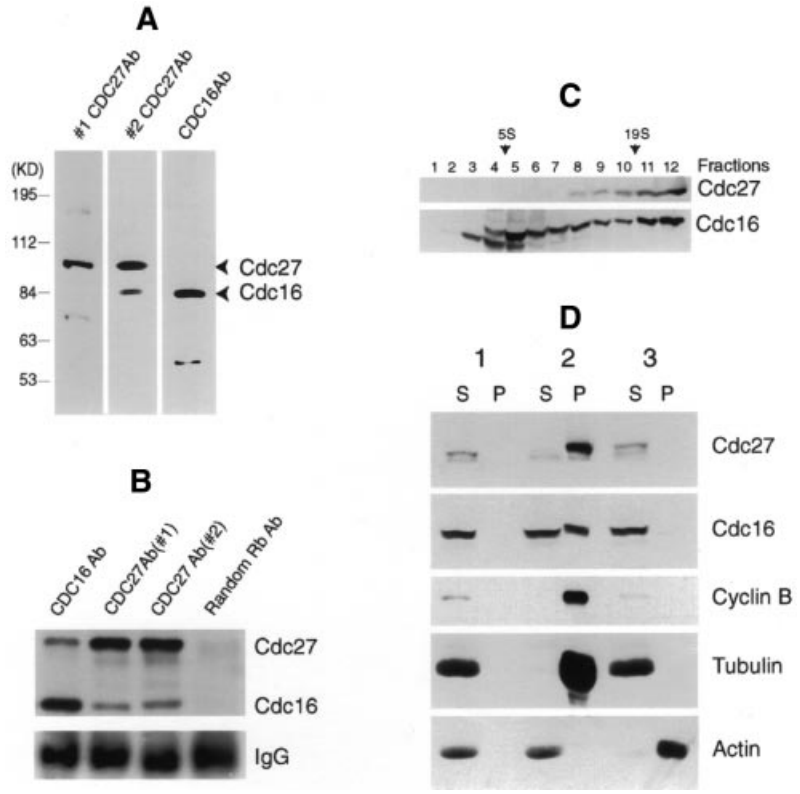

Fig. 7. (**A**) Western blot of embryo extracts probed with affinity-purified antibodies raised against two different anti-Dmcdc27 fusion proteins and one anti-Dmcdc16 fusion protein. (**B**) Immunoprecipitations from embryo extracts, performed with anti-Dmcdc16 antibodies (lane 1), anti-Dmcdc27 antibodies (lanes 2 and 3) or random rabbit IgG (lane 4). The precipitates were analysed by Western blotting with a mixture of anti-Dmcdc16 and anti-Dmcdc27 antibodies. Both Dmcdc16 and Dmcdc27 are precipitated by either the anti-Dmcdc16 or anti-Dmcdc27 antibodies, while neither protein is precipitated by the random IgG. The amount of IgG loaded in each lane is shown as a loading control. Control precipitations were also performed under dissociating conditions (1 M NaCl), and this inhibited the co-precipitation of Dmcdc16 with Dmcdc27 and vice versa (not shown). (**C**) Embryo extracts were separated on a sucrose gradient and blotted with either anti-Dmcdc27 or anti-Dmcdc16 antibodies. (**D**) Western blot of a microtubule spin-down experiment performed with a high-speed supernatant from 0- to 3-h-old embryos and probed with various affinity-purified antibodies (labelled at the right of the figure). S = supernatant, P = pellet. Lane 1: a control experiment where no taxol was added and no microtubules formed; none of the proteins pellet in the absence of microtubules. Lane 2: after the addition of taxol, tubulin is found in the pellet, as are significant fractions of Dmcdc16, Dmcdc27 and cyclin B. Lane 3: after the addition of phalloidin, only actin is found in the pellet.

and that the disappearance of the protein is regulated spatially within the cell.

The dynamic distribution of cyclin B

For our results to be meaningful, the behaviour of the cyclin B–GFP fusion protein must reflect accurately the behaviour of the endogenous cyclin B protein. We found that cyclin B–GFP is partially degraded at the end of mitosis in syncytial embryos with kinetics similar to the endogenous cyclin B (Figure 1B). The distribution of cyclin B–GFP in cellularized embryos, however, differs significantly from the distribution previously reported for cyclin B in formaldehyde-fixed cellularized embryos, where cyclin B was largely cytoplasmic (Lehner and O'Farrell, 1990; Whitfield *et al*., 1990). We find, however, that the endogenous cyclin B in methanol-fixed embryos, stained with affinity-purified anti-cyclin B antibodies, has a very similar distribution pattern to that of cyclin B–GFP in living embryos. The only significant difference is that the accumulation of the endogenous cyclin B in the nucleus prior to NEB and on the centrosomes in mitosis is less pronounced in the fixed embryos. The similarity between the distribution of cyclin B–GFP in living embryos and the endogenous cyclin B in methanol-fixed embryos suggests that cyclin B–GFP is likely to be a reasonably accurate reporter of the behaviour of cyclin B in living cells.

We investigated why the distribution of cyclin B–GFP in living embryos is slightly different from the distribution of the endogenous cyclin B in methanol-fixed embryos, and is very different from the distribution of the endogenous cyclin B in formaldehyde-fixed embryos. We fixed cyclin B–GFP-expressing embryos with either formaldehyde or methanol and stained them with anti-cyclin B antibodies to see if the distribution of the cyclin B–GFP was changed by fixation. The distribution of the cyclin B and cyclin B–GFP in these fixed embryos was indistinguishable from the distribution of cyclin B in similarly fixed wild-type embryos, suggesting that cyclin B–GFP is redistributed subtly upon methanol fixation, and is redistributed drastically upon formaldehyde fixation. If the endogenous cyclin B were also redistributed in this way upon fixation, it would explain why the different fixation methods produce such different results.

The distribution of cyclin B–GFP that we observe in living embryos also agrees well with previous reports on the subcellular distribution of mammalian cyclin B1 in fixed cells (Pines and Hunter, 1991; Jackman *et al*., 1995) and of a cyclin B1–GFP fusion protein in living mammalian cells at particular stages of the cell cycle (the

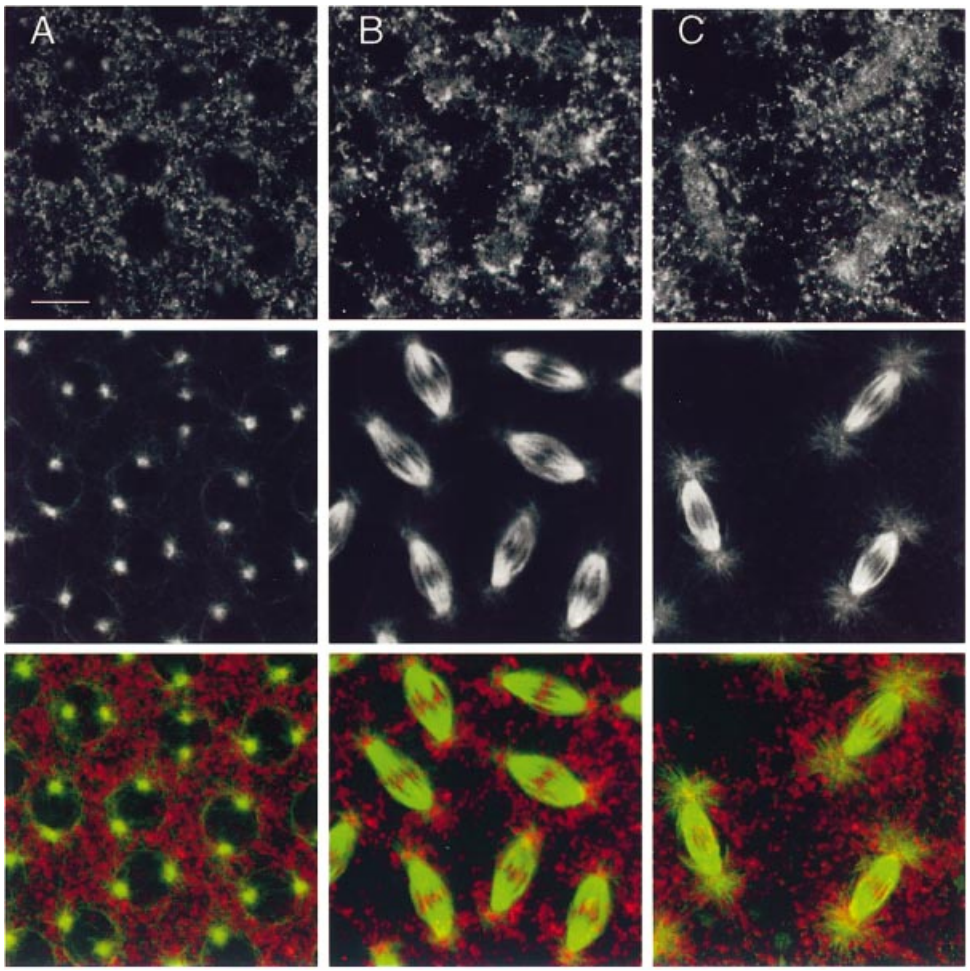

Fig. 8. The distribution of Dmcdc16 and Dmcdc27 in methanol-fixed embryos. The staining of microtubules is shown in the middle panels, Dmcdc16 in the top panels (A and B), Dmcdc27 in the top panel (C) and a merged image in the bottom panels. Both APC/C proteins have a very similar distribution throughout the cell cycle, so only one is shown at each cell cycle stage. In interphase (**A**), metaphase (**B**) and anaphase (**C**), most of the Dmcdc16 and Dmcdc27 appear to be distributed in a punctate pattern throughout the cytoplasm. In some embryos, a weak staining of the centrosomes or spindle region is also seen, and a weak punctate staining is also apparent in the region of the condensed chromatin in the merged images. Scale bar = 10 μm.

long cell cycle and photosensitivity of these cells has so far precluded following the behaviour of cyclin B–GFP throughout an entire cell cycle in a single mammalian cell; Hagting *et al*., 1998). Thus, the gradual accumulation of cyclin B on centrosomes in interphase, the accumulation of the protein in the nucleus prior to nuclear envelope breakdown and the binding of the protein to the mitotic spindle all appear to be conserved features of the protein's behaviour. The striking accumulation of cyclin B that we observe on the plus ends of the interpolar microtubules which overlap in the middle of the spindle has not, however, been reported previously. We suspect that this distribution is also conserved, but it may be particularly easy to observe in *Drosophila* spindles, which are composed mainly of interpolar microtubules. Most mammalian spindles have far fewer interpolar microtubules (Mastronarde *et al*., 1993), which may make the accumulation of cyclin B there harder to see. We do not know the functional significance, if any, of this accumulation, but keeping cdk1–cyclin B activity high in this area may serve to prevent these overlapping microtubules from starting to slide past each other (as is thought to occur in anaphase B) prior to the initiation of chromosome segregation during anaphase A. As the destruction of cyclin B is also required for cytokinesis (Wheatley *et al*., 1997), the concentration of cdk1–cyclin B activity in the middle of the spindle might help prevent the premature initiation of cytokinesis.

The spatially regulated disappearance of cyclin B

We show that the disappearance of cyclin B–GFP from the cell is regulated spatially. In cellularized embryos, the protein associated with the spindle disappears toward the end of metaphase in a wave that spreads from the spindle poles to the spindle equator. When the spindle-associated cyclin B–GFP is almost undetectable, cells enter anaphase, and the remaining cytoplasmic cyclin B–GFP disappears over the next few minutes. It is unclear, however, whether this spatially regulated disappearance of cyclin B–GFP directly reflects the degradation of the protein. Quantitation experiments show that as the protein disappears from the spindle it cannot be detected accumulating anywhere else in the cell, suggesting that the protein is being degraded in the cell at the same time as it is disappearing from the spindle. The simplest interpretation of this result is that the disappearance of cyclin B–GFP from the spindle

directly reflects its degradation, although other explanations are possible (see below).

In syncytial embryos, biochemical studies have shown that cyclin B is only partially degraded at the end of mitosis (Edgar *et al*., 1994). Unfortunately, it was not possible to follow the behaviour of cyclin B–GFP at high resolution in syncytial embryos as the fluorescent signal was very low. As Western blotting revealed that the cyclin B–GFP fusion protein was present in these syncytial embryos (Figure 1B), we suspect that the rapid turnover of the protein (which occurs every 8–10 min in early syncytial embryos; see Figure 1B) means that most cyclin B–GFP molecules do not survive long enough for the GFP moiety to undergo the internal molecular rearrangements required for it to become fluorescent (~30–60 min; Brand, 1995; Hazelrigg *et al*., 1998). Thus, it may well be technically impossible to obtain high resolution images of cyclin B–GFP in syncytial embryos. We found that in methanol-fixed syncytial embryos, however, the disappearance of the endogenous cyclin B followed a pattern similar to that observed with cyclin B–GFP in living cellularized embryos, and the protein started to disappear from the poles of the spindle in late metaphase, and was essentially gone from the spindle by early anaphase (Figure 6). In contrast to the situation in cellularized embryos, however, the levels of cyclin B in the cytoplasm did not change significantly during the latter stages of mitosis, suggesting that, in syncytial embryos, only the cyclin B in the vicinity of the spindle is being degraded.

How might the spatially regulated disappearance of cyclin B be controlled? We speculate that in cellularized embryos the spindle-associated cyclin B is targeted specifically for destruction by the APC/C toward the end of metaphase. This fraction of the cyclin B is then either degraded on the spindle, or is released from the spindle and rapidly degraded in the cytoplasm, while the cytoplasmic cyclin B–GFP is targeted independently for destruction by the APC/C slightly later in mitosis. We favour this explanation for several reasons. First, we find that the APC/C can associate specifically with microtubules *in vitro*, but it appears to be present at multiple sites in the cell: on centrosomes, spindles, chromosomes and in the cytoplasm. Thus, different fractions of the APC/C could be activated independently to target different fractions of cyclin B for destruction in a temporally and spatially regulated manner. Secondly, this scheme could explain how cyclin B can be only partially destroyed at the end of mitosis in syncytial embryos: if only the APC/C associated with the spindles is activated in these embryos, then only the cyclin B in the vicinity of the spindle would be destroyed, which is consistent with what we observe. Thirdly, the spatially regulated activation of the APC/C could explain how in fused tissue culture cells that contain two spindles the activation of the spindle assembly checkpoint in one spindle (by the presence of an unattached kinetochore) does not block the other spindle from exiting mitosis with normal timing (Rieder *et al*., 1997). If our model can be extrapolated to mammalian cells, then the degradation of the spindle-associated cyclin B could be controlled in a spindle-autonomous manner. Moreover, in the fused cell experiments, the checkpoint-arrested spindle is eventually driven into anaphase even if it contains an unattached kinetochore. This result might be expected from our model, as once the APC/C on the spindle is activated to degrade the spindle-associated cyclin B, the APC/C in the cytoplasm could then be activated to degrade the cytoplasmic cyclin B; this fraction of the APC/C could diffuse through the cell and might then degrade the cyclin B on the nearby spindle, allowing it to exit mitosis.

How might the activation of the APC/C to degrade cyclin B be regulated spatially? Recent experiments suggest that the temporal control of APC/C activation toward specific substrates depends on its association with members of the *fizzy (fzy)*/CDC20 and *fizzy-related (fzr)*/CDH1 family of proteins (reviewed in Townsley and Ruderman, 1998). In *Drosophila*, for example, *fzy* is required for the destruction of cyclin A, cyclin B and cyclin B3 at around metaphase/anaphase, whereas *fzr* is required for the destruction of these proteins in late mitosis/G_1 (Sigrist and Lehner, 1997). Perhaps the spatial regulation of cyclin B destruction is also regulated by the association of the APC/C with members of this family of proteins: APC/C–fzy complexes might accumulate on the spindle and ubiquitinate the spindle-associated cyclin B toward the end of metaphase, for example, while APC/C–fzr complexes might remain in the cytoplasm and ubiquitinate the cytoplasmic cyclin B later in mitosis. In syncytial embryos, fzr might not be present or might be inactivate, explaining why only the spindle-associated cyclin B is degraded. Although fzy and fzr have not been seen associated with specific organelles in *Drosophila* embryos (Dawson *et al*., 1995; Sigrist and Lehner, 1997), a fraction of the $p55^{CDC}$ protein, a fzy/CDC20 family member, appears to be located on centrosomes and spindles in mammalian cells (Kallio *et al*., 1998).

If our interpretation that the disappearance of cyclin B–GFP directly reflects its degradation is correct, then our results suggest that a substantial fraction of cyclin B is being degraded while the cell is still in metaphase. This contradicts the prevailing idea that cyclin B is degraded abruptly at the metaphase–anaphase transition. Recent experiments studying the disappearance of cyclin B–GFP fusion proteins in mammalian cells (P.Clute and J.Pines, personal communication) and in *S.pombe* (M.Yanagida, personal communication), however, have also concluded that a substantial fraction of the cyclin B–GFP disappears from cells while they are in metaphase, and this disappearance also appears to be regulated spatially in these systems.

While the spatially regulated activation of the APC/C is an attractive way to explain the spatially regulated disappearance of cyclin B, there are other possible explanations. The degradation of cyclin B, for example, could be initiated in the cytoplasm, but the release of cyclin B from the spindle might initially maintain a relatively constant level of the protein in the cytoplasm. This explanation, however, would not easily account for the partial degradation of cyclin B that is observed in syncytial embryos. Another possibility is that the APC/C is activated globally in the cell to target cyclin B for destruction, but it is concentrated on the spindle in metaphase and then moves into the cytoplasm during the latter stages of mitosis. This explanation is not consistent with our observations on the localization of Dmcdc16 and Dmcdc27 in fixed embryos, but this localization may not reflect accurately the distribu-

tion of these proteins in living cells. It is also possible that the targeting of cyclin B for degradation and the degradation itself may be separable events: the protein may be polyubiquitinated by the APC/C on the spindle, for example, but it may have to leave the spindle to be degraded by the 26S proteosome. More experiments will be required to analyse how the spatially regulated disappearance of cyclin B that we observe is related to its polyubiquitination and ultimate degradation. Moreover, it has been shown recently that cyclin B is not essential for mitosis in cellularized embryos if cyclin B3 is present (Jacobs *et al*., 1998). Cyclin B3 appears to be a nuclear protein; it will be interesting to investigate how cyclin B3 compensates for the loss of cyclin B.

The disappearance of cyclin B is initiated at the spindle poles: implications for the spindle assembly checkpoint

None of the models discussed above explain why the disappearance of cyclin B initiates at the spindle poles and spreads toward the spindle equator. This observation is consistent with the previous demonstration that there is a wave of histone dephosphorylation along the chromosomes during anaphase in early *Drosophila* embryos which spreads from the kinetochores, which lead the chromosomes toward the spindle poles, to the telomeres (Su *et al*., 1998). Our results suggest that this wave of dephosphorylation may reflect directly the earlier inactivation of cdk1–cyclin B activity spreading from the spindle poles to the equator.

It is unclear how such a wave of cyclin B disappearance could be generated. Perhaps polo-like kinases are involved in this process. These kinases have multiple functions during the cell cycle (Golsteyn *et al*., 1996; Glover *et al*., 1998), and they are located at multiple sites in the cell, including the centrosomes at metaphase and the spindle midbody during late mitosis (Golsteyn *et al*., 1995; Adams *et al*., 1998; Logarinho and Sunkel, 1998; Wianny *et al*., 1998). These kinases can activate the APC/C (Descombes and Nigg, 1998; Kotani *et al*., 1998; Shirayama *et al*., 1998), and they can associate with a kinesin-like protein (Lee *et al*., 1995; Adams *et al*., 1998). Perhaps a centrosomal polo kinase initially activates the APC/C at the centrosome, and a kinesin then transports the kinase toward the spindle equator, enabling the kinase to activate a wave of cyclin B destruction.

Recently, much attention has focused on the role of unattached kinetochores in activating the spindle assembly checkpoint (reviewed in Wells, 1996; Rieder and Salmon, 1998). This checkpoint seems to involve the inhibition of the APC/C by the Mad2 checkpoint protein (Fang *et al*., 1998) and, as discussed above, it appears to be spindle autonomous (Rieder *et al*., 1997). Our results suggest that the spindle pole may also play an important part in regulating the exit from mitosis. This raises the interesting possibility that the checkpoint signal generated from an unattached kinetochore might need to be transmitted to the spindle pole to prevent the initiation of cyclin B destruction. While such a model is highly speculative, we note that the Mad2 protein is found both on unattached kinetochores and on centrosomes in mammalian cells (Gorbsky *et al*., 1998). Perhaps the Mad2 protein can travel along the microtubules within a spindle, communicating the status of the kinetochores to the spindle poles, explaining why an unattached kinetochore can only block the exit from mitosis within its own spindle.

Materials and methods

Construction of cyclin B–GFP

The cDNA encoding full-length *Drosophila* cyclin B in Bluescript pKS (pKS-CycB) was modified by PCR with high fidelity *Taq* (Boehringer Mannheim) so that the stop codon was replaced by a *Bam*HI site (pKS-CycBB). The coding region of mGFP6 (Schuldt *et al*., 1998) was amplified by PCR to contain a *Bam*HI site in-frame with the cyclin B cDNA and an *Spe*I site at its 3′ end. This fragment was subcloned into pKS-CycBB, creating the vector pKS-CycB-GFP. The CycB-GFP insert was cut out with *Kpn*I and *Spe*I, and subcloned into the pWR-PUbq transformation vector (Nick Brown, personal communication), which placed cyclin B–GFP under the control of the polyubiquitin promoter. The same insert was also subcloned into the Dm277 transformation vector (Micklem *et al*., 1997) that placed the cyclin B–GFP under the control of the maternal (67C) α-tubulin promoter. Flies were transformed with these constructs using standard techniques (Roberts, 1986); eight independent PUbq-CycB-GFP lines and 10 independent α-tubulin (67C)-CycB-GFP lines were obtained. Lines containing multiple copies of the cyclin B–GFP transgenes were obtained using standard genetic crosses (Roberts, 1986). All data presented here were obtained with one of these lines that contained four copies of the PUbq-CycB-GFP transgene.

Analysis of live embryos

Cyclin B–GFP embryos were dechorionated by hand and mounted on a coverslip on a small amount of glue that had been dissolved in heptane and painted in a stripe on the coverslip. The embryos were covered in voltalef oil and were observed with a Bio-Rad MRC 1024 confocal system mounted on an inverted Nikon microscope. Images were converted to PCT format and imported into Adobe Photoshop 4.0, where they were adjusted to use the full range of pixel intensities. The images were then imported into Adobe Premier 4.2, where they were made into movies.

Quantitation of the levels of cyclin B–GFP at the various locations in the cell was carried out using NIH Image 1.61. The mean pixel intensity in a small (10×10 pixel) area was calculated, and this was repeated four to eight times at different points in each location of the cell (cytoplasm, nucleus, spindle, mid-spindle) for each image. The results were averaged and were then normalized (to allow for any bleaching of the GFP signal) by comparing the mean pixel intensity at each time point in the cytoplasm of a nearby cell that had remained in interphase throughout the period of observation (usually 4–6 min). A background factor was subtracted from these figures to allow for the fact that when a cell has its lowest levels of cyclin B–GFP fluorescence (usually 3–4 min after cytokinesis is complete) it does not have a mean pixel intensity of zero. This was calculated by averaging the pixel intensity in the cytoplasm of a nearby cell at a time when it had reached its lowest level of fluorescence. Thus, the zero point on the *y*-axis of Figure 3 represents the lowest level of cyclin B–GFP fluorescence that occurs in a cell, rather than a pixel intensity of zero.

Embryo fixation and antibody staining

Embryos were fixed in 95% methanol/5% 0.25 M EGTA and processed for indirect immunofluoresence staining as described previously (Kellogg *et al*., 1988). Embryos were fixed with formaldehyde using either a 4% formaldehyde solution supplemented with taxol to preserve the microtubules (Gonzalez and Glover, 1993), or a neat (40%) formaldehyde solution (Theurkauf and Hawley, 1992) that also preserves microtubules. Tubulin was detected with DM1a antibody (Sigma; 1/500 dilution). Affinity-purified anti-cyclin B, anti-Dmcdc16 and anti-Dmcdc27 antibodies were used at 1–2 μg/ml. DNA was detected with propidium iodide as described previously (Gonzalez and Glover, 1993). Images were collected on a Bio-Rad MRC 1024 confocal microscope, and imported into Adobe Photoshop 4.0. The images were adjusted to use the full range of pixel intensities, and in some cases an unsharp mask filter was applied to the whole image.

Cloning of Dmcdc16

Degenerate oligonucleotides were designed to regions of the cdc16 protein that were conserved between human, *Saccharomyces cerevisiae* and *S.pombe* (full details available upon request). These were used to amplify DNA by PCR from *Drosophila* genomic DNA. Bands of the

expected size were generated and used to screen a λ Zap *Drosophila* embryonic cDNA library (Carl Thummel, personal communication). Several cDNAs were isolated, the longest of which was 2.6 kb. This cDNA was sequenced on both strands using an ABI prism dye termination kit. Sequencing gels were run at the DNA sequencing facility in the Department of Genetics, University of Cambridge, UK. The sequence confirmed that this cDNA encoded the *Drosophila* homologue of cdc16. This sequence has been submitted to the DDBJ/EMBL/GenBank databases under accession No. AF105333.

Preparation and purification of antibodies

Antibodies were raised in rabbits against maltose-binding protein (MBP) fusion proteins (New England Biolabs). The following fusions were used: MBP–CycB, containing amino acids 2–304 of cyclin B; MBP–cdc27#1, containing amino acids 674–875 of Dmcdc27; MBP–cdc27#2, containing amino acids 140–420 of Dmcdc27; and MBP–cdc16, containing amino acids 416–746 of Dmcdc16. All fusion proteins were purified according to the manufacturer's instructions, and antigen injections and sera production were performed by Eurogentec (Belgium). Antibodies were purified against the relevant fusion protein that had been covalently coupled to either Affigel 10, Affigel 15 (Bio-Rad) or Amino-link (Pierce) resins. Immune sera were first depleted of anti-MBP antibodies by passing each serum repeatedly over an Amino-link–MBP column until no anti-MBP antibodies remained. Specific antibodies were then purified by passing each serum over the appropriate column of MBP fusion protein. The column was washed extensively with phosphate-buffered saline (PBS) with 0.5 M KCl, and antibodies were eluted in 0.1 M glycine, pH 2.1. The antibodies were neutralized with 1 M Tris pH 8.5. Glycerol was added to 50%, and the antibodies were stored at –20°C. Affinity-purified antibodies were used in all the experiments reported here.

Analysis of protein behaviour

The expression of cyclin B and cyclin B–GFP in embryos was analysed by fixing 2- to 4-h-old embryos in methanol. Twenty embryos were rehydrated, transferred into SDS sample buffer (Laemmli, 1970) and boiled for 10 min before being fractionated by SDS–PAGE, blotted to nitrocellulose and probed with the appropriate antibodies. The expression of Dmcdc16 and Dmcdc27 was analysed in 0- to 24-h-old embryos in the same way. Embryos that were to be sorted by cell cycle stage were rehydrated, stained with 4′,6-diamidino-2-phenylindole (DAPI) and sorted on a fluorescent microscope.

Immunoprecipitation (IP) experiments were performed on extracts from 0- to 3-h-old embryos as described previously (Kidd and Raff, 1997). Control IPs were performed using dissociating conditions (C buffer plus 1 M NaCl). Sucrose gradient sedimentation of embryo extracts was performed as described previously (Raff *et al*., 1993), except that experiments were performed without the addition of 0.5 M KCl to the extract or to the gradient. Fractions from the gradient were separated by SDS–PAGE, blotted onto nitrocellulose and probed with the appropriate antibodies. Microtubule spin-down experiments were performed as described previously (Raff *et al*., 1993).

Western blotting was performed as described previously (Towbin *et al*., 1979); all primary antibodies were used at 1–2 μg/ml, and blots were developed using an enhanced chemiluminescence kit (ECL) from either Amersham or Pierce. Quantitation of blots was performed using NIH Image 1.61.

Acknowledgements

We thank Jon Pines, Paul Clute and Mitsuhiro Yanagida for communicating their results prior to publication, and Jon Pines for many useful and stimulating discussions. We thank Stuart Tugendreich and Phil Hieter for generously providing the Dmcdc27 cDNA clone, Carl Thummel for providing a cDNA library, and Fanni Gergely, Kim Jeffers, James Wakefield and Jon Pines for helpful comments on the manuscript. This work was funded by a Senior Research Fellowship in Basic Biomedical Sciences from the Wellcome Trust.

References

Adams,R.R., Tavares,A.A., Salzberg,A., Bellen,H.J. and Glover,D.M. (1998) *pavarotti* encodes a kinesin-like protein required to organize the central spindle and contractile ring for cytokinesis. *Genes Dev.*, **12**, 1483–1494.

Alfa,C.E., Ducommun,B., Beach,D. and Hyams,J.S. (1990) Distinct nuclear and spindle pole body population of cyclin–cdc2 in fission yeast. *Nature*, **347**, 680–682.

Brand,A. (1995) GFP in *Drosophila*. *Trends Genet*., **11**, 324–325.

Charles,J.F., Jaspersen,S.L., Tinker-Kulberg,R.L., Hwang,L., Szidon,A. and Morgan,D.O. (1998) The Polo-related kinase Cdc5 activates and is destroyed by the mitotic cyclin destruction machinery in *S.cerevisiae*. *Curr. Biol.*, **8**, 497–507.

CohenFix,O., Peters,J.M., Kirschner,M.W. and Koshland,D. (1996) Anaphase initiation in *Saccharomyces cerevisiae* is controlled by the APC dependent degradation of the anaphase inhibitor Pds1p. *Genes Dev.*, **10**, 3081–3093.

Dawson,I.A., Roth,S. and Artavanis-Tsakonas,S. (1995) The *Drosophila* cell cycle gene *fizzy* is required for normal degradation of cyclins A and B during mitosis and has homology to the *CDC20* gene of *Saccharomyces cerevisiae*. *J. Cell Biol.*, **129**, 725–737.

Debec,A. and Montmory,C. (1992) Cyclin B is associated with centrosomes in *Drosophila* mitotic cells. *Biol. Cell*, **75**, 121–126.

Descombes,P. and Nigg,E.A. (1998) The polo-like kinase Plx1 is required for M phase exit and destruction of mitotic regulators in *Xenopus* egg extracts. *EMBO J.*, **17**, 1328–1335.

Edgar,B.A., Sprenger,F., Duronio,R.J., Leopold,P. and O'Farrell,P.H. (1994) Distinct molecular mechanisms regulate cell cycle timing at successive stages of *Drosophila* embryogenesis. *Genes Dev.*, **8**, 440–452.

Fang,G., Yu,H. and Kirschner,M.W. (1998) The checkpoint protein MAD2 and the mitotic regulator CDC20 form a ternary complex with the anaphase-promoting complex to control anaphase initiation. *Genes Dev.*, **12**, 1871–1883.

Foe,V.E. (1989) Mitotic domains reveal early commitment of cells in *Drosophila* embryos. *Development*, **107**, 1–22.

Funabiki,H., Kumada,K. and Yanagida,M. (1996) Fission yeast *cut1* and *cut2* are essential for sister chromatid separation, concentrate along the metaphase spindle and form large complexes. *EMBO J.*, **15**, 6617–6628.

Glotzer,M., Murray,A.W. and Kirschner,M.W. (1991) Cyclin is degraded by the ubiquitin pathway. *Nature*, **349**, 132–138.

Glover,D.M., Hagan,I.M. and Tavares,A.A.M. (1998) Polo-like kinases: a team that plays throughout mitosis. *Genes Dev.*, **12**, 3777–3787.

Golsteyn,R.M., Mundt,K.E., Fry,A.M. and Nigg,E.A. (1995) Cell cycle regulation of the activity and subcellular localization of Plk1, a human protein kinase implicated in mitotic spindle function. *J. Cell Biol.*, **129**, 1617–1628.

Golsteyn,R.M., Lane,H.A., Mundt,K.E., Arnaud,L. and Nigg,E.A. (1996) The family of polo-like kinases. *Prog. Cell Cycle Res.*, **2**, 107–114.

Gonzalez,C. and Glover,D.M. (1993) Techniques for studying mitosis in *Drosophila*. In Fantes,P. and Brooks,R. (eds), *The Cell Cycle*. Oxford University Press, Oxford, UK, pp. 143–174.

Gorbsky,G.J., Chen,R.H. and Murray,A.W. (1998) Microinjection of antibody to Mad2 protein into mammalian cells in mitosis induces premature anaphase. *J. Cell Biol.*, **141**, 1193–1205.

Hagting,A., Karlsson,C., Clute,P., Jackman,M. and Pines,J. (1998) MPF localization is controlled by nuclear export. *EMBO J.*, **17**, 4127–4138.

Harper,J.W. and Elledge,S.J. (1996) Cdk inhibitors in development and cancer. *Curr. Opin. Genet. Dev.*, **6**, 56–64.

Hazelrigg,T., Liu,N., Hong,Y. and Wang,S. (1998) GFP expression in *Drosophila* tissues: time requirements for formation of a fluorescent product. *Dev. Biol.*, **199**, 245–249.

Hershko,A., Ganoth,D., Sudakin,V., Dahan,A., Cohen,L.H., Luca,F.C., Ruderman,J.V. and Eytan,E. (1994) Components of a system that ligates cyclin to ubiquitin and their regulation by the protein kinase cdc2. *J. Biol. Chem.*, **269**, 4940–4946.

Irniger,S., Piatti,S., Michaelis,C. and Nasmyth,K. (1995) Genes involved in sister chromatid separation are needed for B type cyclin proteolysis in budding yeast. *Cell*, **81**, 269–278.

Jacobs,H.W., Knoblich,J.A. and Lehner,C.F. (1998) *Drosophila* cyclin B3 is required for female fertility and is dispensable for mitosis like cyclin B. *Genes Dev.*, **12**, 3741–3751.

Jackman,M., Firth,M. and Pines,J. (1995) Human cyclins B1 and B2 are localized to strikingly different structures: B1 to microtubules, B2 primarily to the Golgi apparatus. *EMBO J.*, **14**, 1646–1654.

Jorgensen,P.M., Brundell,E., Starborg,M. and Hoog,C. (1998) A subunit of the anaphase-promoting complex is a centromere-associated protein in mammalian cells. *Mol. Cell Biol.*, **18**, 468–476.

Juang,Y.L., Huang,J., Peters,J.M., McLaughlin,M.E., Tai,C.Y. and Pellman,D. (1997) APC-mediated proteolysis of Ase1 and the morphogenesis of the mitotic spindle. *Science*, **275**, 1311–1314.

Kallio,M., Weinstein,J., Daum,J.R., Burke,D.J. and Gorbsky,G.J. (1998) Mammalian p55CDC mediates association of the spindle checkpoint protein Mad2 with the cyclosome/anaphase-promoting complex and is involved in regulating anaphase onset and late mitotic events. *J. Cell Biol.*, **141**, 1393–1406.

Kellogg,D.R., Mitchison,T.J. and Alberts,B.M. (1988) Behaviour of microtubules and actin filaments in living *Drosophila* embryos. *Development*, **103**, 675–686.

Kidd,D. and Raff,J.W. (1997) LK6, a short lived protein kinase in *Drosophila* that can associate with microtubules and centrosomes. *J. Cell Sci.*, **110**, 209–219.

King,R.W., Peters,J.H., Tugendreich,S., Hieter,P., Rolfe,M. and Kirschner,M.W. (1995) A 20S complex containing cdc27 and cdc16 catalyzes the mitosis specific conjugation of ubiquitin to cyclin B. *Cell*, **81**, 279–288.

King,R.W., Deshaies,R.J., Peters,J.M. and Kirschner,M.W. (1996) How proteolysis drives the cell cycle. *Science*, **274**, 1652–1659.

Kotani,S., Tugendreich,S., Fujii,M., Jorgensen,P.M., Watanabe,N., Hoog,C., Hieter,P. and Todokoro,K. (1998) PKA and MPF-activated polo-like kinase regulate anaphase-promoting complex activity and mitosis progression. *Mol. Cell*, **1**, 371–380.

Laemmli,U.K. (1970) Cleavage of the structural proteins during the assembly of the head of bacteriophage T4. *Nature*, **227**, 680–685.

Lee,H.S., Simon,J.A. and Lis,J.T. (1988) Structure and expression of ubiquitin genes of *Drosophila melanogaster*. *Mol. Cell. Biol.*, **8**, 4727–4735.

Lee,K.S., Yuan,Y.L., Kuriyama,R. and Erikson,R.L. (1995) Plk is an M-phase-specific protein kinase and interacts with a kinesin- like protein, CHO1/MKLP-1. *Mol. Cell Biol.*, **15**, 7143–7151.

Lehner,C.F. and O'Farrell,P.H. (1990) The roles of *Drosophila* cyclins A and B in mitotic control. *Cell*, **61**, 535–547.

Lew,D.J. and Kornbluth,S. (1996) Regulatory roles of cyclin dependent kinase phosphorylation in cell cycle control. *Curr. Opin. Cell Biol.*, **8**, 795–804.

Logarinho,E. and Sunkel,C.E. (1998) The *Drosophila* POLO kinase localises to multiple compartments of the mitotic apparatus and is required for the phosphorylation of MPM2 reactive epitopes. *J. Cell Sci.*, **111**, 2897–2909.

Maldonado-Codina,G. and Glover,D.M. (1992) Cyclins A and B associate with chromatin and the polar regions of spindles, respectively and do not undergo complete degradation at anaphase in syncytial *Drosophila* embryos. *J. Cell Biol.*, **116**, 967–976.

Mastronarde,D.N., McDonald,K.L., Ding,R. and McIntosh,J.R. (1993) Interpolar spindle microtubules in PTK cells. *J. Cell Biol.*, **123**, 1475–1489.

Michaelis,C., Ciosk,R. and Nasmyth,K. (1997) Cohesins: chromosomal proteins that prevent premature separation of sister chromatids. *Cell*, **91**, 35–45.

Micklem,D.R., Dasgupta,R., Elliott,H., Gergely,F., Davidson,C., Brand,A., Gonzalez-Reyes,A. and St. Johnston,D. (1997) The *mago nashi* gene is required for the polarisation of the oocyte and the formation of perpendicular axes in *Drosophila*. *Curr. Biol.*, **7**, 468–478.

Murray,A. (1995) Cyclin ubiquitination the destructive end of mitosis. *Cell*, **81**, 149–152.

Pines,J. and Hunter,T. (1991) Human cyclins A and B1 are differentially located in the cell and undergo cell cycle-dependent nuclear transport. *J. Cell Biol*, **115**, 1–17.

Raff,J.W., Kellogg,D.R. and Alberts,B.M. (1993) *Drosophila* gamma tubulin is part of a complex containing two previously identified centrosomal MAPs. *J. Cell Biol.*, **121**, 823–835.

Riabowol,K., Draitta,G., Brizuila,L., Vandre,D. and Beach,D. (1989) The cdc2 kinase is a nuclear protein that is essential for mitosis in mammalian cells. *Cell*, **57**, 393–401.

Rieder,C.L. and Salmon,E.D. (1998) The vertebrate cell kinetochore and its roles during mitosis. *Trends Cell. Biol.*, **8**, 310–318.

Rieder,C.L., Khodjakov,A., Paliulis,L.V., Fortier,T.M., Cole,R.W. and Sluder,G. (1997) Mitosis in vertebrate somatic cells with two spindles: implications for the metaphase/anaphase transition checkpoint and cleavage. *Proc. Natl Acad. Sci. USA*, **94**, 5107–5112.

Roberts,D. (1986) *Drosophila*: *A Practical Approach*. IRL Press, Oxford, UK.

Schuldt,A.J., Adams,J.H., Davidson,C.M., Micklem,D.R., Haseloff,J., Johnston,D.S. and Brand,A.H. (1998) Miranda mediates asymmetric protein and RNA localization in the developing nervous system. *Genes Dev.*, **12**, 1847–1857.

Shirayama,M., Zachariae,W., Ciosk,R. and Nasmyth,K. (1998) The Polo-like kinase Cdc5p and the WD-repeat protein Cdc20p/fizzy are regulators and substrates of the anaphase promoting complex in *Saccharomyces cerevisiae*. *EMBO J.*, **17**, 1336–1349.

Sigrist,S.J. and Lehner,C.F. (1997) *Drosophila* fizzy-related down-regulates mitotic cyclins and is required for cell proliferation arrest and entry into endocycles. *Cell*, **90**, 671–681.

Su,T.T., Sprenger,F., DiGregorio,P.J., Campbell,S.D. and O'Farrell,P.H. (1998) Exit from mitosis in *Drosophila* syncytial embryos requires proteolysis and cyclin degradation and is associated with localized dephosphorylation. *Genes Dev.*, **12**, 1495–1503.

Theurkauf,W.E. and Hawley,R.S. (1992) Meiotic spindle assembly in *Drosophila* females: behavior of nonexchange chromosomes and the effects of mutations in the nod kinesin-like protein. *J. Cell Biol.*, **116**, 1167–1180.

Towbin,H., Staehlin,T. and Gordon,J. (1979) Electrophoretic transfer of proteins from polyacrylamide gels to nitrocellulose sheets: procedures and some applications. *Proc. Natl Acad. Sci. USA*, **80**, 4350–4354.

Townsley,F.M. and Ruderman,J.V. (1998) Proteolytic ratchets that control progression through mitosis. *Trends Cell Biol.*, **8**, 238–243.

Tugendreich,S., Tomkiel,J., Earnshaw,W. and Hieter,P. (1995) Cdc27hs colocalizes with cdc16hs to the centrosome and mitotic spindle and is essential for the metaphase to anaphase transition. *Cell*, **81**, 261–268.

Wells,W.A.E. (1996) The spindle assembly checkpoint: aiming for a perfect mitosis, every time. *Trends Cell Biol.*, **6**, 228–234.

Wheatley,S.P., Hinchcliffe,E.H., Glotzer,M., Hyman,A.A., Sluder,G. and Wang,Y. (1997) CDK1 inactivation regulates anaphase spindle dynamics and cytokinesis *in vivo*. *J. Cell Biol.*, **138**, 385–393.

Whitfield,W.G.F., Gonzalez,C., Maldonado-Codina,G. and Glover,D.M. (1990) The A- and B-type cyclins of *Drosophila* are accumulated and destroyed in temporally distinct events that define separable phases of the G_2–M transition. *EMBO J.*, **9**, 2563–2572.

Wianny,F., Tavares, Evans,M.J., Glover,D.M. and Zernicka-Goetz,M. (1998) Mouse polo-like kinase 1 associates with the acentriolar spindle poles, meiotic chromosomes and spindle midzone during oocyte maturation. *Chromosoma*, **107**, 430–439.

Yamada,H., Kumada,K. and Yanagida,M. (1997) Distinct subunit functions and cell cycle regulated phosphorylation of 20S APC/cyclosome required for anaphase in fission yeast. *J. Cell Sci.*, **110**, 1793–1804.

Received February 4, 1999; revised and accepted March 2, 1999